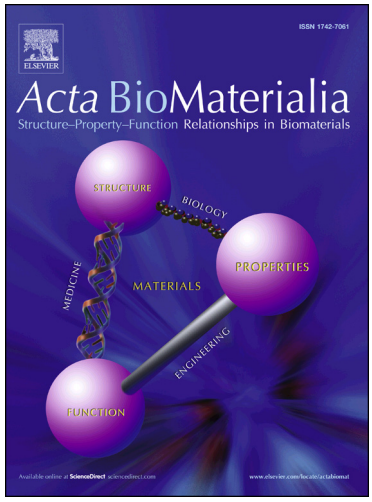

Full length article

The effect of biomimetic calcium deficient hydroxyapatite and sintered β-tricalcium phosphate on osteoimmune reaction and osteogenesis

Joanna M. Sadowska, Fei Wei, Jia Guo, Jordi Guillem-Marti, Zhengmei Lin, Maria-Pau Ginebra, Yin Xiao

PII: S1742-7061(19)30479-9
DOI: https://doi.org/10.1016/j.actbio.2019.06.057
Reference: ACTBIO 6233

To appear in: *Acta Biomaterialia*

Received Date: 19 February 2019
Revised Date: 25 June 2019
Accepted Date: 27 June 2019

Please cite this article as: Sadowska, J.M., Wei, F., Guo, J., Guillem-Marti, J., Lin, Z., Ginebra, M-P., Xiao, Y., The effect of biomimetic calcium deficient hydroxyapatite and sintered β-tricalcium phosphate on osteoimmune reaction and osteogenesis, *Acta Biomaterialia* (2019), doi: https://doi.org/10.1016/j.actbio.2019.06.057

The effect of biomimetic calcium deficient hydroxyapatite and sintered β-tricalcium phosphate on osteoimmune reaction and osteogenesis.

Joanna M. Sadowska[1,2,‡], Fei Wei[3], Jia Guo[3,4], Jordi Guillem-Marti[1,2],Zhengmei Lin[4], Maria-Pau Ginebra[1,2,5], Yin Xiao[3]**

[1]Biomaterials, Biomechanics and Tissue Engineering Group, Department of Materials Science and Metallurgical Engineering, Universitat Politècnica de Catalunya (UPC), Av. Eduard Maristany 16, 08019 Barcelona, Spain.

[2]Barcelona Research Centre in Multiscale Science and Engineering, Universitat Politècnica de Catalunya (UPC), Av. Eduard Maristany 16, 08019 Barcelona, Spain.

[3]Institute of Health and Biomedical Innovation and the Australia-China Centre for Tissue Engineering and Regenerative Medicine (ACCTERM), Queensland University of Technology, Brisbane, QLD 4059, Australia

[4]Guanghua School of Stomatology, Hospital of Stomatology, Sun Yat-sen University and Guanghua Provincial Key Laboratory of Stomatology, Guangzhou, Guangdong, 510055, People's Republic of China

[5]Institute for Bioengineering of Catalonia (IBEC), The Barcelona Institute of Science and Technology, Baldiri Reixac 10-12, 08028 Barcelona Spain.

[‡]Current address: Tissue Engineering Research Group (TERG), Dept. of Anatomy, Royal College of Surgeons in Ireland (RCSI), 123 St. Stephen's Green, Dublin 2, Ireland.

E-mail addresses: joannasadowska@rcsi.com (J.M. Sadowska), f2.wei@hdr.qut.edu.au (F. Wei), guojia5@mail2.sysu.edu.cn (J. Guo), jordi.guillem.marti@upc.edu (J. Guillem-Marti), linzhm@mail.sysu.edu.cn (Z. Lin), maria.pau.ginebra@upc.edu (M-P. Ginebra), yin.xiao@qut.edu.au (Yin Xiao)

*Corresponding authors:

Maria-Pau Ginebra

Biomaterials, Biomechanics and Tissue Engineering Department

Department of Materials Science and Metallurgical Engineering

Universitat Politècnica de Catalunya

Avinguda Eduard Maristany 16, 08019, Barcelona, Spain

Tel: +34 934017706

Email: maria.pau.ginebra@upc.edu

Yin Xiao

Institute of Health and Biomedical Innovation,

Queensland University of Technology,

60 Musk Ave, Kelvin Grove, Brisbane, Queensland 4059, Australia

Tel: +61 7 31386240

Email: yin.xiao@qut.edu.au

ABSTRACT. Biomaterial implantation triggers inflammatory reactions. Understanding the effect of physicochemical features of biomaterials on the release of inflammatory cytokines from immune cells would be of great interest in view of designing bone graft materials to enhance the healing of bone defects. The present work investigated the interactions of two chemically and texturally different calcium phosphate (CaPs) substrates with macrophages, one of the main innate immune cells, and its further impact on osteogenic differentiation of bone forming cells. The behaviour of macrophages seeded on biomimetic calcium deficient hydroxyapatite (CDHA) and sintered β-tricalcium phosphate (β-TCP) was assessed in terms of the release of inflammatory cytokines and osteoclastogenic factors. The osteogenic differentiation of bone progenitor cells (bone marrow stromal cells (BMSCs) and osteoblastic cell line (SaOS-2)) were subsequently studied by incubating with the conditioned medium induced by macrophage-CaPs interaction in order to reveal the effect of immune cell reaction to CaPs on osteogenic differentiation. It was found that the incubation of macrophages with CaPs substrates caused a decrease of pro-inflammatory cytokines, more pronounced for β-TCP compared with CDHA showing significantly decreased IL-6, TNF-a, and iNOS. However, the macrophage-CDHA interaction resulted in a more favourable environment for osteogenic differentiation of osteoblasts with more collagen type I production and osteogenic genes (Runx2, BSP) expression, suggesting that osteogenic differentiation of bone cells is not only determined by the nature of biomaterials, but also significantly influenced by the inflammatory environment generated by the interaction of immune cells and biomaterials.

KEYWORDS: osteoimmunomodulation, immunomodulation, inflammation, calcium phosphates, osteogenesis

1. INTRODUCTION

The initial tissue reaction after implantation of a biomaterial is the inflammatory response provoked in the host, which largely determines biomaterial's long-term performance [1–4]. The inflammatory host response involves the activation of numerous cell types. Among them, the innate immune responses, such as macrophage polarization to either pro-inflammatory M1 or anti-inflammatory M2 phenotypes, with the consequent release of a wide range of mediator molecules [5,6], will result in different healing pathways.

In general, as a first step, the implantation of synthetic bone graft leads to the activation of M1 phenotype, which is coupled with the release of pro-inflammatory cytokines (mainly interleukin 6, IL-6; interleukin 1, IL-1 and tumour necrosis factor alpha (TNFα)) and reactive species intermediates (reactive oxygen species (ROS) and nitric oxide synthase (NOS)). This induces the necessary inflammatory phase, resulting in the recruitment of progenitors and immune cells. In another hand the chemoattractants and cytokines released in this phase can also stimulate the process of osteoclastogenesis [7,8]. Furthermore, prolonged presence of the pro-inflammatory M1 phenotype produces chronic inflammation, including the expression of fibrous agents and granuloma formation and finally resulting in implant encapsulation and failure [9]. Therefore, the effective and timely switch from pro-inflammatory M1 to anti-inflammatory M2 phenotype will contribute to active bone tissue regeneration as the secretion of anti-inflammatory cytokines such as interleukin 10 (IL-10) is critical in bone forming environment [10] regulating osteogenic differentiation of bone cells [11,12]. In general, the functionality of macrophages and thus their cytokine release profile is tightly linked to local environmental stimuli. The high plasticity of

immune cells has fostered the development of different strategies to control macrophage polarization [9]. For instance, the exposure to microbial products such as lipopolysaccharide (LPS) activates M1 phenotype and is frequently applied to assess the anti- inflammatory capacity of biomaterials [13].

Recently, the possibility to modulate macrophage polarisation by tuning biomaterial properties has attracted increasing attention. For instance, it has been shown that the functionality and polarization of immune cells can be influenced by chemical [14–19] or topographical [18–22] properties of biomaterials. Understanding how the macrophage-biomaterial interaction is translated into osteoclastic and osteogenic events would be of great interest in view of designing synthetic bone grafts with tailored features to foster bone formation.

In this context, CaPs are particularly relevant, since they are common bone substitutes due to the similarity to inorganic fraction of bone [23-28]. The ionic exchange they promote with the extracellular fluids, and more specifically, their ability to locally decrease the concentration of calcium and phosphate ions, associated in some instances with the formation of an apatite layer, has been proposed to be one of the triggering mechanisms for their intrinsic osteoinductive potential [29]. In this context, the effect of CaPs on immune [30,31], osteoclastic [32-36] or bone forming cells [37] have been widely investigated. Among the innate immune cells, the macrophages were reported to actively participate in the host-cell response to CaPs materials. They trigger mesenchymal stem cells (MSCs) migration, making them strong mediators in bone formation process [38]. Nevertheless, there is still some knowledge gap regarding the effect of the inflammatory environment created after CaPs implantation, on osteoclastogenesis and osteogenesis processes. Although recent findings highlighted the role of some physicochemical properties of CaPs on modulating osteoimmune responses [39,40], the studies were limited to

sintered ceramics such as β-tricalcium phosphate (β-TCP). Recently, biomimetic calcium phosphates, which are obtained at low temperature and have structural and compositional features much closer to the mineral phase of bone, were shown to have enhanced osteoinductive and osteogenic properties [25–27]. Moreover, their structural features can be easily modified during synthesis process which allows obtaining biomimetic CaPs with various topographies from nano to micro range and triggers specific cell response. For instance, we previously demonstrated that bringing the topography of biomimetic calcium deficient hydroxyapatite (CDHA) to nanoscale resulted in stimulation of osteogenic activities of bone forming cells whilst the increase of porosity of CDHA positively modulated its anti-inflammatory capacity [41].

In present work, we aim to study the interplay between the inflammatory environment generated by the features of CaPs and the process of osteogenesis. The biomimetic CDHA is subjected to a thermal treatment in order to obtain sintered β-TCP ceramic with similar Ca/P ratio and porosity but different topography and crystallographic features. In this way we can compare the immunomodulatory effects of two CaPs which differ not only chemically but also texturally, *i.e.* plate-like crystals of CDHA vs. polyhedral grains of β-TCP. The inflammatory regulation and osteogenic capacity of biomimetic CDHA and a conventional β-TCP ceramic were assessed through evaluation of the release of inflammatory, osteoclastogenic factors from immune cells, as well as the subsequent effect on bone cell differentiation.

2. MATERIALS AND METHODS

2.1. Material preparation and characterisation

The synthesis of biomimetic CDHA and β-TCP samples was previously described [42,43]. Briefly, CDHA discs were prepared through a cementitious reaction using an α-tricalcium

phosphate (α-TCP). The solid phase was a mixture of α-TCP powder and 2 wt.% of precipitated hydroxyapatite (PHA; Merck 2143, Merck, Darmstardt, Germany). The solid phase was mixed with a liquid phase that consisted of 2.5 wt.% disodium hydrogen phosphate (Na_2HPO_4; Panreac), at a 0.35 mL/g liquid-to-powder ratio (L/P). The paste was placed in Teflon moulds of 2 mm of height and 6 mm of diameter. The samples were immersed in water at 37 ˚C for 7 days to allow for complete reaction. The β-TCP discs were obtained by sintering the CDHA discs at 1100 ˚C for 15 h.

The microstructure of CDHA and β-TCP was assessed through scanning electron microscopy (SEM; TESKAN MIRA3). Prior to visualisation, thin layer of gold was deposited on samples using EM SC005 Gold Coater (Leica). To determine the surface roughness of samples, the area of 47.5 x 63.4 μm^2 was scanned using optical interferometry (Veeco Wyko NT1100) and a 50x magnification. Images were acquired using Vision32 software.

2.2. Cell culture

In current study three models of cells were used: the murine macrophages (RAW 264.7 cells), human osteosarcoma (SaOS-2) and human BMSCs. RAW 264.7 and SaOS-2 were expanded in Dulbecco's Modified Eagle Medium (DMEM; Gibco®, Life Technologies Pty Ltd., Australia Life Technologies) supplemented with penicillin/streptomycin (50 U/ml and 50 μg/ml, respectively), (P/S; Gibco®, Life Technologies Pty Ltd., Australia Life Technologies) and heat-inactivated foetal calf serum (FCS; *In Vitro* Technologies, Australia FCS). Cells were maintained at 37°C with a 5% CO_2 humidified incubator.

The BMSCs were isolated and cultured following the protocols established in previous reports [18,44,45]. Briefly, bone marrow was obtained from 50-60 year old patients undergoing knee or

hip replacement. The informed consent was given from all donors and the procedure was approved by the Ethics Committee of Queensland University of Technology. The isolation of mononuclear cells from bone marrow was performed adding Lymphoprep (Axis-Shield PoC AS, Oslo, Norway) following the manufacturer's instructions. Subsequently, the cells were transferred to culture flasks with DMEM with 10% of FCS and penicillin/streptomycin (50 U/ml and 50 µg/ml, respectively). Unattached hematopoietic cells were removed via medium changes. BMSCs in passage 4-5 were used in the current study.

2.3. Response of macrophages to CaPs substrates under inflammatory environment

For sterilization, the CaPs samples were immersed in 80% of ethanol. Subsequently, three washings with phosphate-buffered saline (PBS, Oxoid) were performed and the discs were then left overnight in complete DMEM. Afterwards, the $7x10^5$ RAW cell/cm^2 were seeded directly on substrates. The anti-inflammatory performance of CaPs substrates was studied by activating the M1 proinflammatory phenotype of macrophages with LPS treatment [13,18]. Briefly, the cell culture medium was replaced after 12 h with medium containing 1 µg/mL of LPS (LPS, *Escherichia coli* 055:B5, R&D Systems). After 2h of incubation, LPS-containing medium was aspirated, samples were rinsed thrice with PBS and transferred to a new well plate. The RAW cells on CaPs substrates were then cultured additional 6 hours in serum-fee cell culture medium. Subsequently, the CaPs-RAW conditioned medium were recovered for further experiments with BMSCs and SaOS-2 cells. Unless otherwise stated, the following experimental procedures were applied to LPS-stimulated RAW cells. The macrophage cells cultured on tissue culture polystyrene (TCPS) or glass coverslip (CS) and exposed to LPS stimulation are labelled as "control+" whilst the RAW cells cultured on TCPS or CS with standard cell culture DMEM media are labelled as "control".

2.4. RAW cells morphology

The morphological characteristics of macrophages cultured in direct contact with CaP discs was evaluated using SEM (TESKAN MIRA3). Briefly, cells were washed with PBS and fixed with 3% glutaldehyde at 4^{o}C for 1 h. The process was followed by three risings with PBS and post-fixation with 1% osmium tetraoxide for 1h. Subsequently, samples were incubated with increasing concentrations of ethanol (50%, 70%, 90%, 100%). Complete dehydration was achieved adding hexamethyldisilazane (HMDS, Sigma-Aldrich). A thin gold layer was deposited on samples using EM SC005 Gold Coater (Leica) and they were visualised by SEM using 5 kV of an acceleration voltage.

The morphology of macrophages was additionally visualised using confocal microscopy (CLSM; Nikon A1) staining cells for F-actin, nuclei and nitric oxide synthase (iNOS). Cells were washed with PBS and fixed with 4% paraformaldehyde (PFA, Sigma-Aldrich) in PBS for 30 min. Then, cells were permeabilized with 0.1 % Triton X- 100 (Merck) in PBS for 15 min and blocked with 1% bovine serum albumin (BSA, Sigma-Aldrich) in PBS for 1h. Cells were then incubated with rabbit polyclonal anti-iNOS in 1% BSA (1:100, Abacam) for 1h. Afterwards, cells were incubated with Alexa Fluor488 Conjugate anti-rabbit IgG (1:1000, Cell Signaling Technology, Danvers, MA) and rhodamine phalloidin in 0.1% Triton X-100 in PBS for 1 h (1:300) in the dark. The nuclei were counterstained through 2 min incubation with 4, 6-diamidino-2-phenylindole (DAPI, Molecular Probes) (1:1000) in 0.1 % Triton X- 100 in PBS. Each step during all procedure was followed by 3x washings with 0.15% glycine in PBS. Images were treated with Fiji/ImageJ package [46] and cell spreading, iNOS area and cell elongation ratio were determined semiquantitatively (n=20).

In parallel, RAW morphology on CaPs was also evaluated without LPS activation incubating RAW cells with CaPs substrates up to 3 days. Cell morphology was determined at day 1 and 3 through staining for F-actin and nuclei. Cell number was determined through nuclei counting using Fiji/Image-J package. Cell number was compared to control group (RAW seeded on glass coverslip) in order to discard cytotoxic effects of CaPs substrates. Moreover, the metabolic activity of RAW cells cultured on CaP substrates was evaluated at days 1 and 3 following a previously described protocol [41].

2.5. Inflammatory and osteoclastogenic behaviour of macrophages

To evaluate gene expression, cells were lysed and total RNA was obtained using TRIzol reagent (Ambion™, Life Technologies Pty Ltd., AustraliaLife Technologies) following the provider protocols at specified cell culture time. The total RNA concentration was determined by NanoDrop ND-1000 spectrophotometer (NanoDrop technologies, Motchanin, DE, USA). Subsequently, 1000 ng of total RNA were reverse transcribed using DyNAmo™ cDNA Synthesis Kit (Genesearch, QLD, Australia). The cDNA template was amplified with the Quantstudio TM Real-Time PCR machine (Applied Biosystems, Foster City, California, USA) using SYBR Green qPCR Master Mix (Life Technologies). The inflammatory RAW response to CaPs was determined analysing the gene expression of pro-inflammatory (IL-1β, IL-6, TNFα, iNOS) and anti-inflammatory (IL-10 and CD206) cytokines and surface markers. Osteoclastogenic activities of macrophages on CaPs were determined measuring the expression CAR2, CTSK and MMP9. The sequences of primers are listed in Table 1. The specificity of primers was determined by analysis of melt curves. The mean cycle threshold (Ct) value of each target gene was normalized against the Ct value of the endogenous control 18S. In order to compare the effect of two different chemistries of CaPs, the using comparative Ct ($2^{-\Delta\Delta CT}$)

method was applied where ΔΔCt= (Ct_{sample} (gene of interest) - Ct_{sample} (endogenous reference gene)) – (Ct_{TCPS} (gene of interest) – Ct_{TCPS} (housekeeping gene)) [47]. Control+ was used as a calibrator sample.

Table 1 Primers' sequences used in this study

	Gene	**Gene symbol**	**Primer' sequences (5' to 3')**
Houskeeping gene	18S ribosomal RNA	*18S*	F:CGGAACTGAGGCCATGATTAAG R:GTATCTGATCGTCTTCGAACCTCC
Pro-inflamatory	Interleukin 1 beta	*Il-1β*	F:TGGAGAGTGTGGATCCCAAG R:GGTGCTGATGTACCAGTTGG
	Interleukin 6	*Il-6*	F:ATAGTCCTTCCTACCCCAATTTCC R:GATGAATTGGATGGTCTTGGTCC
	Tumor necrosis factor alpha	*Tnfα*	F:CTGAACTTCGGGGTGATCGG R:GGCTTGTCACTCGAATTTTGAGA
	Nitric oxide synthase	*inos*	F: CACCAAGCTGAACTTGAGCG R:CGTGGCTTTGGGCTCCTC
Anti-inflammatory	Interleukin 10	*Il-10*	F:CAGGACTTTAAGGGTTACTTG R:ATTTTCACAGGGGAGAAATC
	Mannose receptor C type	*Cd206*	F:AGACGAAATCCCTGCTACTG R:CACCCATTCGAAGGCATTC
Osteoclastogenesis	Cathepsin K	*Ctsk*	F:CCAGTTTTACAGCAGAGGTGTG R:CTTGCTTCCCTTCTGGGTG
	Carbonic	*Car2*	F:AGCAGCGAGCAGATGTCTC

	anhydrase 2		R:TGAGCTGGACGCCAGTTG
	Matrix metallopeptidase 9	*Mmp9*	F:GGGCGTGTCTGGAGATTCG R:CACCTGGTTCACCTCATGGTC
Osteogenesis	Runt-related transcription factor 2	*RUNX2*	F:GACGAGGCAAGAGTTTCACC R:ATGAAATGCTTGGGAACTGC
	Bone morphogenic protein 2	*BMP-2*	F:TGCCATTGTTCAGACGTTGG R:GTACTAGCGACACCCACAAC
	Bone sialoprotein	*BSP*	F:TTTCTGCTACAACACTGGGCTATG R: TTGTTATATCCCCAGCCTTCTTG
	Osteocalcin	*OCN*	F:GCAAAGGTGCAGCCTTTGTG R:GGCTCCCAGCCATTGATACAG
	Collagen type I	*COLL I*	F:AGAACAGCGTGGCCT R:TCCGGTGTGACTCGT

Moreover, the cytokine release was analysed using enzyme-linked immunosorbent assay (ELISA). Specifically, the presence of IL-6, TNF-α and IL-10 was evaluated using a mouse IL-6 Uncoated ELISA kit, a mouse TNF-α Uncoated ELISA kit and a mouse IL-10 Uncoated ELISA kit respectively (all from Invitrogen).

2.6. Measurement of ion concentration of cell culture medium

The concentration of Ca^{2+} and P_i, with and without presence of RAW cells on CaPs, was evaluated in the medium using inductively coupled plasma-optical emission spectrometry (ICP-OES, Perkin Elmer, MA, USA). Prior to analysis, the sample supernatants were diluted fivefold with 2% of ultrapure nitric acid (Sigma-Aldrich).

2.7. The effect of CaPs- RAW conditioned media on osteogenesis

The effect of the microenvironment created by the immune cells cultured on CaP substrates on osteogenesis was determined by incubating bone-forming cells with CaPs-RAW conditioned extracts. Briefly, BMSCs and SaOS-2 cells were separately seeded on tissue culture plastic (TCPS) at densities of $1x10^4$ cells/cm^2 and $2.5x10^4$ cells/cm^2, respectively. After 12h of adhesion, the CaPs-RAW extract previously supplemented with 10% of FCS was added. The BMSCs and SaOS-2 cells were exposed to CAPs-RAW extracts up to three days without medium change. Additionally, the SaOS-2 cells were also seeded on the CaPs discs and exposed to CaPs-RAW conditioned or CaP- conditioned extracts. Afterwards, the expression of osteogenesis-related genes (ALP, Runx2, COLL I, BSP, BMP-2 and OCN) was determined following the protocol described in section 2.5. The values of gene expression were normalised to 18S as a housekeeping gene and BMSCs+ and SaOS-2+ groups were used as a calibrator samples. Over following manuscript "BMSCs+" and "SaOS-2+" refers to respectively mesenchymal and osteoblastic cells exposed to extracts from LPS-stimulated RAW cells.

Additionally, for SaOS-2 cells, the protein expression was determined through CLSM visualisation (for ALP) and western blot (for ALP, COLL I and Runx2). For CLSM analysis the cells were placed on glass coverslip. Afterwards, standard fixation and staining protocol for CLSM visualisation were applied (section 2.4.). The rabbit anti-human ALP (1:100, Abacam) and Alexa Fluor488 Conjugate anti-rabbit IgG secondary antibody (1:1000, Cell Signaling Technology, Danvers, MA) were used as a primary and secondary antibody, respectively. Images were treated using Fiji/ImageJ package. The cell spreading and elongation ratio as well as the ALP area were determined semiquantitely (n=20) using the same software.

For western blot analysis, cells were lysed with RIPA buffer and total protein was quantified by Pierce™ BCA Protein Assay Kit (Thermo Fisher Scientific). The sodium dodecyl sulfate–polyacrylamide gel electrophoresis (SDS-PAGE) were used to separate 20 µg of proteins. Subsequently, they weretransferred onto a nitrocellulose membrane (Pall Corporation, East Hills, New York, USA) and blocked with Odyssey blocking buffer (LI-COR Biosciences, Lincoln, Nebraska, USA) for 1h. The membrane was incubated overnight at 4^{o}C with antibodies against ALP, Runx2, COLL I or α-tubulin (all 1:1000, rabbit anti-human; Abcam, Cambridge, United Kingdom) followed by incubation with anti-mouse/rabbit IRDye 700/800 conjugated antibody (1:5000, Rockland, Gilbertsville, Pennsylvania, USA). In order to remove non-specific binding, washes with TBS-Tween buffer were performed between each incubation step. The Odyssey infrared imaging system (LI-COR Biosciences, Lincoln, Nebraska, USA) was used to visualise the bands. The intensity of bands was determined through Fiji/ImageJ package.

To quantify mineralization, the semi-confluent $3x10^4$ BMSCs/cm^2 BMSCs and $6x10^4$ SaOS-2 /cm^{2}cells were seeded on TCPS. After 24h, the solution ofCaPs-RAW extracts and DMEM with osteogenic supplements: 50 µg/mL ascorbic acid, 10 mM β-glycerophosphate and 100 nM dexamethasone was added. The medium was replaced every third day. At day 14, the cells were thoroughly rinsed with double distilled H_2O (ddH_2O) and the fixation was performed incubating cells for 15 min at room temperature with 4% PFA. Subsequently, the Alizarin red solution (ARS, Sigma-Aldrich) at pH 4.2 was added and the cells were incubated for 20 min. The unbound stain was eliminated through several rinses with ddH_2O. The samples were air-dried, and the images were acquired using a light microscope (Nikon ECLIPSE TS100).

2.8. Statistical analysis

The statistical analysis was performed using SPSS software (IBM SPSS, Armonk, NewYork, USA). The data was plotted as mean ± standard deviation (SD). The normality was checked through the Saphiro–Wilk test. In case of significance of Saphiro-Wilk test, the statistical differences between groups was determined by Mann-Whitney U test. In case of non-significant Saphiro-Wilk test, the statistical differences between groups was determined by T-Student test. For all tests, the level of significance was set for $p < 0.05$.

3. RESULTS

3.1. Physicochemical characterisation of CaPs

SEM micrographs showed that the microstructure of biomimetic CDHA was formed of aggregates with plate- like crystals and average roughness (Ra) of 2.5 ± 0.72 μm. The sintering process applied to β-TCP led to coalescence of crystals within CDHA aggregates, resulting in polyhedral grain microstructure (Figure 1) and lower Ra being 1.33 ± 0.23 μm. Further characterisation regarding substrates' SSA and porosity was described in a previous work [48–50] and displayed in Figure 1C.

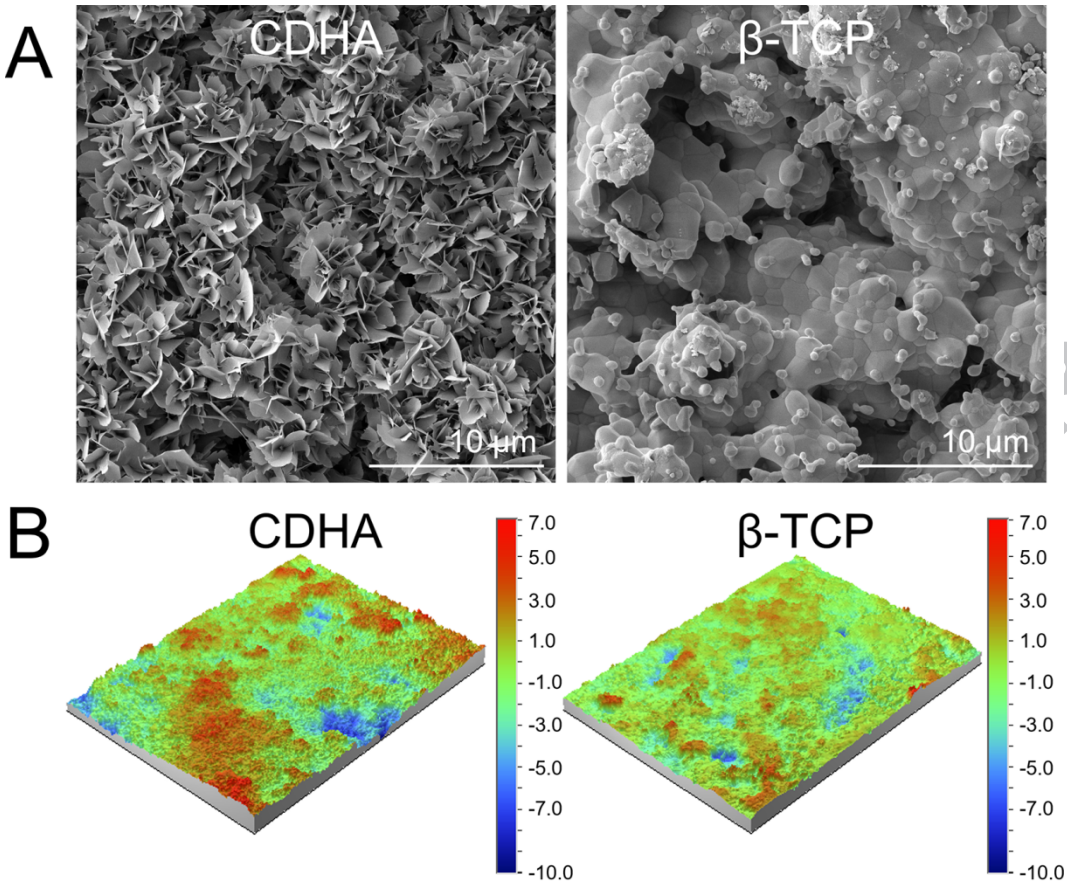

C

Substrate	Nominal Ca/P ratio	Solubility at 25°C (-log(K_s))[51]	Roughness Ra (µm)	SSA (m^2/g)[49]	Porosity (%)[49]
CDHA	1.5	~85.1	2.53± 0.72	14.11± 0.01	33.4
β-TCP	1.5	28.9	1.33± 0.23	0.38 ± 0.00	29.8

Figure 1. A) Representative SEM micrographs of CDHA and β-TCP surface morphology. **B)** Optical interferometry images of surface topography of CDHA and β-TCP substrates. **C)** Physicochemical properties of substrates used in the study [49,51].

3.2. No cytotoxic effect of CaP substrates on the macrophage cell line (RAW cells)

Macrophages adhered at similar numbers on CaP substrates and control. A progressive increase of cell number was observed from day 1 to day 3 of cell culture. β- TCP presented statistically significant higher number of RAW cells at day 3 compared to control (Figure 2A). Moreover, an increase of metabolic activity of macrophages from day 1 to day 3 was observed in all CaPs. Both substrates presented similar values compared to the control group (Figure 2B).

In general, RAW cells cultured on CaPs and control presented a round-shaped morphology (Figure 2B and C). Moreover, macrophage organization into clusters was observed at day 3 for all conditions.

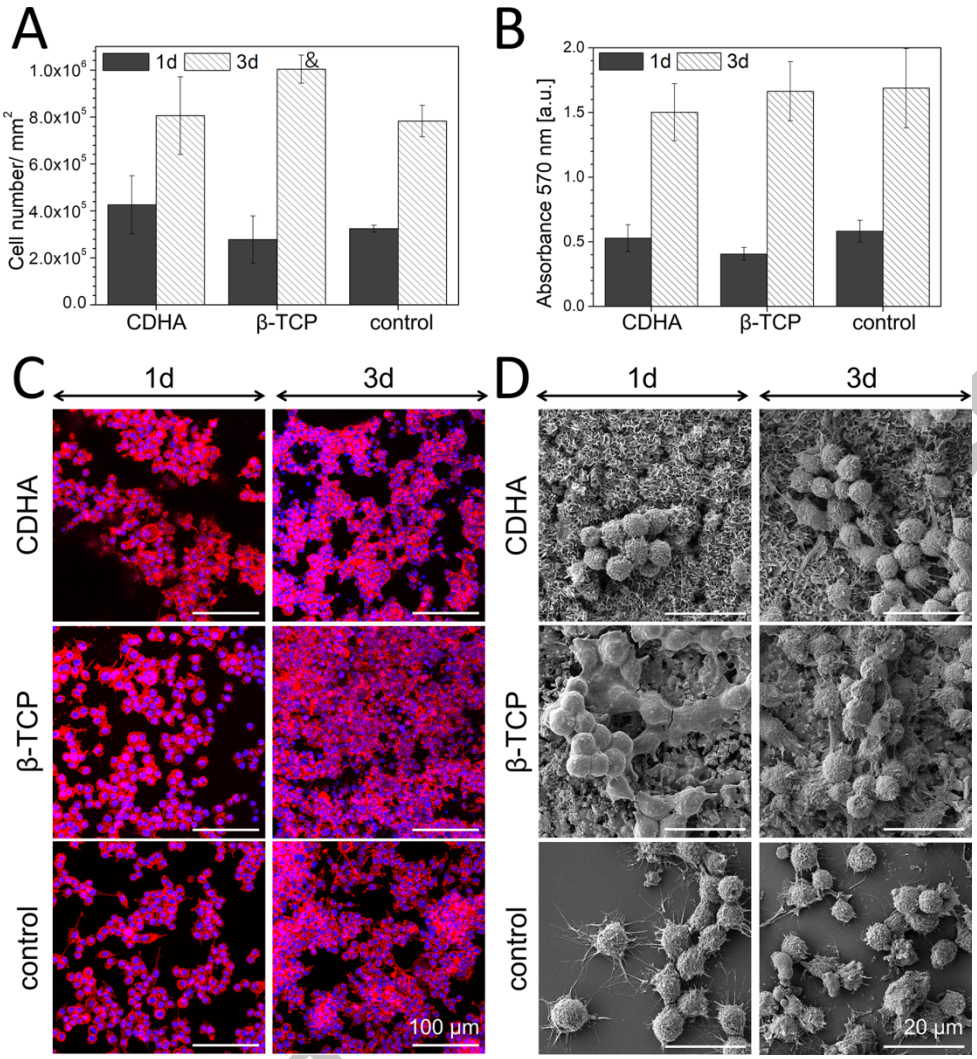

Figure 2. A) The number of attached RAW cells to CaP substrates. The quantification was based on nuclei counting of CLSM images acquired at day 1 and day 3 of cell culture. **B)** Metabolic activity of RAW cells on CaPs substrates detected by MTT. In **A)** and **B)** & indicates statistically significant difference ($p<0.05$) compared to control. No statistically significant difference ($p<0.05$) was observed between CDHA and β-TCP substrate. **C)** CLMS images of macrophages on CaP discs at day 1 and 3 of cell culture. The F-actin (red) and cell nuclei (blue) were stained. The brightness and contrast of images were adjusted using Fiji/Image-J package. **D)** Representative SEM images of morphology of RAW on CaPs at day 1 and 3 of cell culture. In

A), **B)** and **C)** "Control" refers to RAW seeded on glass coverslip while in **D)** "Control" refers to RAW seeded on TCPS.

3.3. CaP substrates could down-regulate the inflammatory response of macrophages under inflammatory conditions

Inflammatory conditions were induced through incubation of RAW cells with LPS. Subsequently, the gene expression and cytokine release of macrophages cultured on CaPs was evaluated in terms of inflammatory, osteoclastic and osteogenic activities.

3.3.1. The inflammatory response of RAW cells cultured on CaPs

The gene expression of pro-inflammatory (IL-1β, IL-6, TNFα and iNOS) and anti-inflammatory (IL-10 and CD206) genes and surface markers are depicted in Figure 4A. In general, the culturing of macrophages on CaPs discs resulted in a downregulation of pro-inflammatory genes compared to control group. These values were approximately 4-fold (for IL-1β and IL-6) and 2-fold (for TNF-α and iNOS) lower compared to control. Moreover, the downregulation of pro-inflammatory molecules was significantly more pronounced on β-TCP than on biomimetic CDHA. No statistically significant differences were observed for the expression of anti-inflammatory cytokine IL-10. However, CaP substrates downregulated the expression of surface marker CD206, more markedly in the case of β-TCP (Figure 3A). Moreover, both substrates decreased the release of pro-inflammatory IL-6 and TNFα being this scenario more pronounced for β-TCP (Figure 3B).

The anti-inflammatory capacity of CaPs was also assessed through iNOS visualisation (Figure 3C). The presence of iNOS-positively stained RAW cells was observed in both CaP substrates.

Nonetheless, β-TCP showed lower iNOS- stained area compared to CDHA and control+ group (Figure 4D, middle graph).

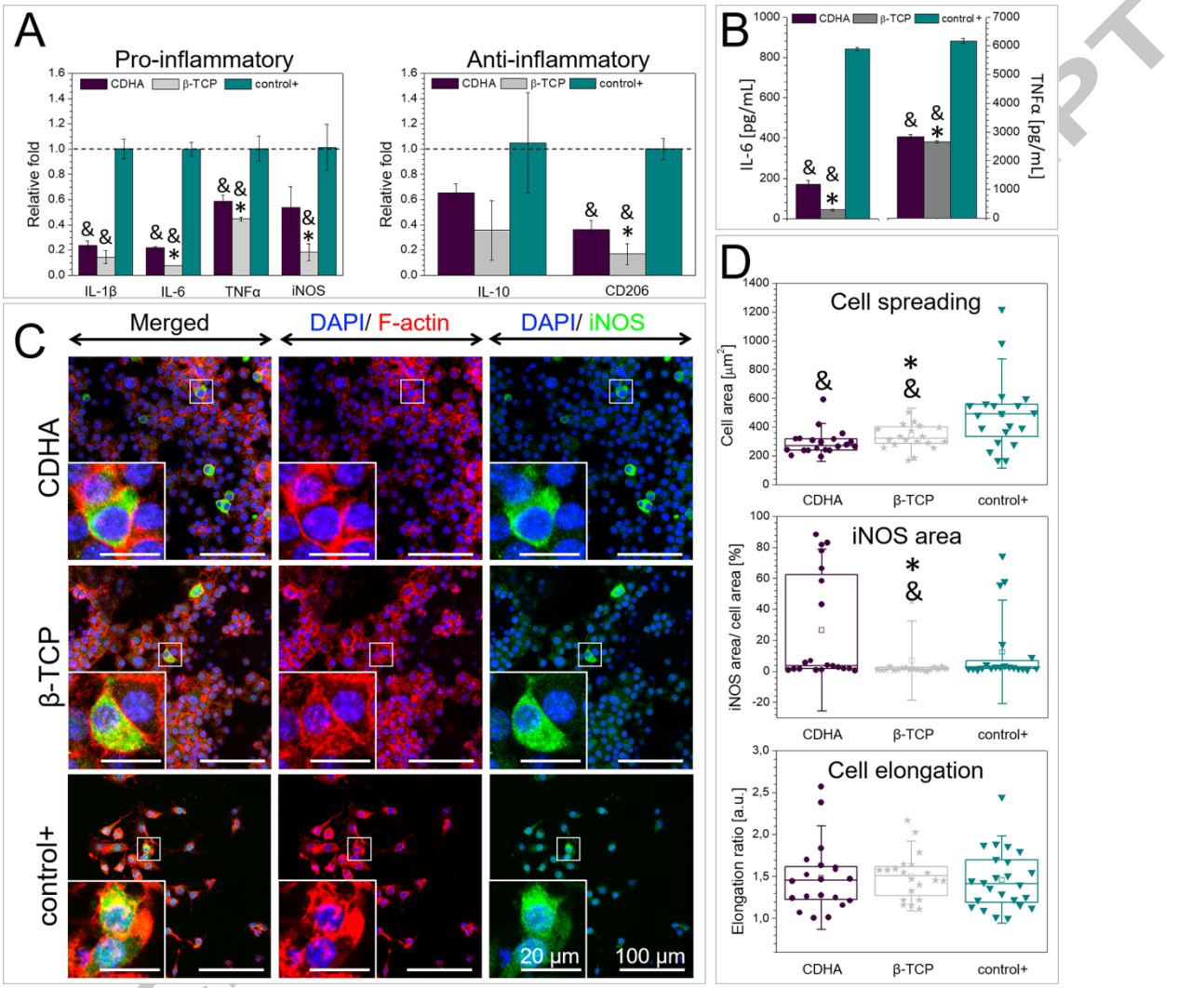

Figure 3. The response of RAW cells to CaP substrates under inflammatory environment (6 hours after LPS stimulation). **A)** Relative expression of pro-inflammatory (left) and anti-inflammatory (right) genes of macrophages cultured on CaP samples. The values were normalised to 18S as a housekeeping gene and using LPS-stimulated macrophages (control+) as a calibrator. The dashed line indicates the relative fold equal to 1. * indicates statistically significant difference ($p<0.05$) of β-TCP substrate compared to CDHA. **B)** Levels of M1 pro-

inflammatory (IL-6 and TNFα) cytokines in cell culture media supernatants. The M2 anti-inflammatory (IL-10) cytokine was not detected [41]. **C)** Representative CLSM images of iNOS-positively stained RAW cells on CaPs. The F-actin (red), cellular nuclei (blue) and iNOS (green) were stained. The brightness and contrast of images were adjusted with Fiji/ImageJ package. **D)** Semiquantitative analysis of RAW spreading, iNOS occupied area and elongation ratio. Symbols represent individual cells (n=20), the boxes represent 25th and 75th percentile, the middle line is the median, the □ is the mean and whiskers are standard deviation. & indicates statistically significant difference ($p<0.05$) compared to control+. * indicates statistically significant difference ($p<0.05$) of β-TCP substrate compared to CDHA.

The elongation ratio and spreading area of cells cultured on CaPs substrates provides an indication of the polarization of macrophages to either pro or anti-inflammatory phenotype (Figure 3C and Figure 4) [52]. RAW cells cultured directly on CaP substrates presented lower spreading area than the control, this being more pronounced for macrophages cultured on CDHA (Figure 3C, top graph). However, similar cell elongation ratios were observed for both substrates (Figure 3C, bottom graph). The cell morphologies observed by SEM were compatible with on β-TCP and CDHA surfaces (Figure 4).

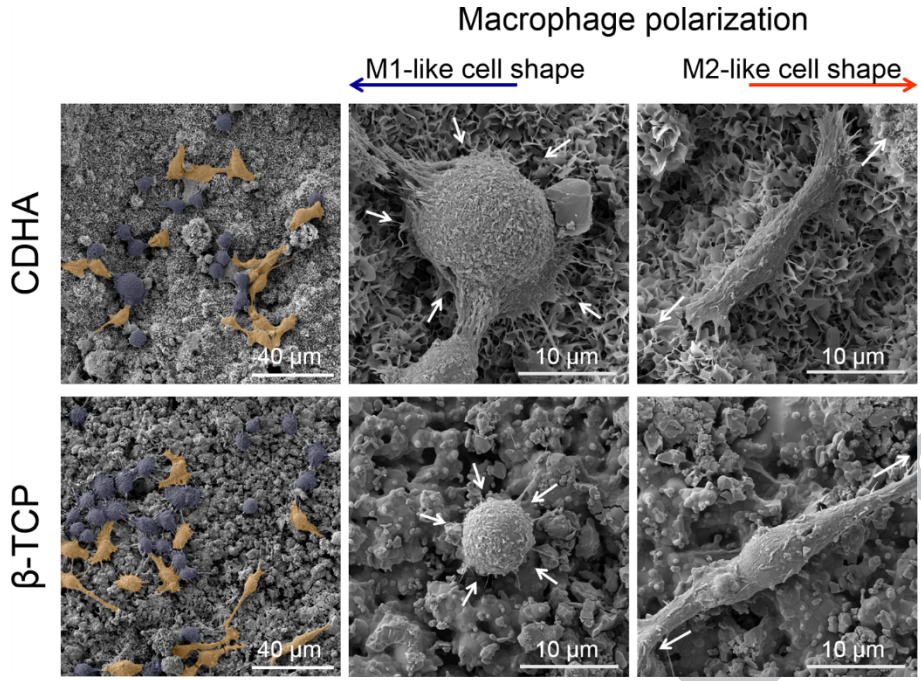

Figure 4. SEM micrographs of morphology of on CaP substrates cultured under inflammatory environment (6 hours after LPS stimulation). Pseudo coloured blue and orange cells indicate macrophages with pancake-like and elongated morphology (*i.e.* M1 and M2-like cell shape), respectively. White arrows show putative direction of spreading of macrophages.

3.3.2. Regulation of osteoclastic-like behaviour of RAW cells by CaPs

The culture of RAW cells on CaP substrates resulted in the downregulation of osteoclastic marker genes (CTSK, CAR2 and MMP9) (Figure 5A). Similar decrease in the expression of CTSK and CAR2 genes was observed for both CDHA and β-TCP, whist the downregulation of MMP9 was more pronounced for β-TCP.

The levels of calcium and phosphate were monitored in presence or absence of cells (Figure 5B). The concentration of Ca^{2+} and P_i in the pristine DMEM were 1.66 ± 0.00 mM and 1.09 ± 0.02 mM, respectively. The immersion of CDHA in the DMEM caused a 17.19 ± 2.60% decrease of

Ca^{2+} concentration, which was counteracted by a slight increase in presence of the RAW cells (Figure 5B, left graph). No alteration in Ca^{2+} concentration was noted for β-TCP. On the other hand, little alterations of phosphate were observed (Figure 5B, right graph) in any of the culture conditions.

The resorptive behaviour of macrophages on CaPs was additionally evaluated through SEM imaging of the cell-material interphase (Figure 5C, left graph). The morphology of the CaP substrate areas adjacent to the RAW cells was similar to the pristine substrate, with no signs of degraded crystals. Few multinucleated cells, which could be associated to a resorptive activity, were found on both CDHA and β-TCP (Figure 5C, right graph).

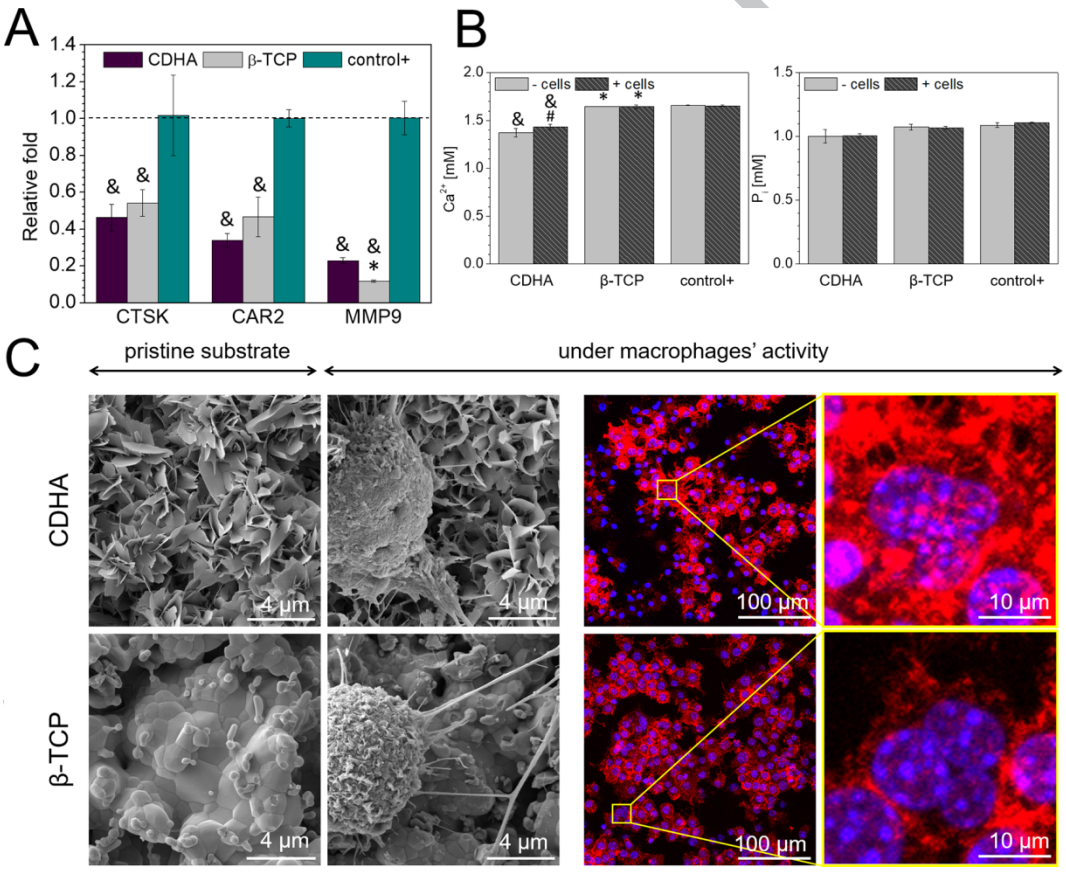

Figure 5. Osteoclastic-like behaviour of RAW on CaPs after 6 hours of LPS- stimulation. **A)** Relative expression of osteoclastogenesis-related genes (CTSK, CAR2 and MMP9) of RAW.

The values were normalised to 18S as a housekeeping gene and using RAW cells after 6 hours of LPS-stimulation (control+) as a calibrator sample. The dashed line indicates the relative fold equal to 1. **B)** Ionic alterations of calcium and phosphate cause by CaP substrates in absence and presence of macrophages. In **A)** and **B)** & and * indicate statistically significant difference ($p<0.05$) compared to control and CDHA, respectively. In **B)** # indicates statistically significant difference ($p<0.05$) between ionic concentration of cell culture medium with or without cells. **C)** Representative SEM and CLSM images of CaPs-RAW interphase (left) and multinucleated macrophages (right). The F-actin (red) and cellular nuclei (blue) were stained. The brightness and contrast of CLSM images were adjusted with Fiji/ImageJ package.

3.4. The impact of osteoimmune environment of RAW cells-CaP interaction on osteogenesis

The ability of macrophages cultured on CaP substrates to stimulate osteogenesis was analysed using RAW-CaPs extracts and assessing the capacity of the macrophage-secreted molecules to induce the osteogenic differentiation of BMSCs and SaOS-2.

Stimulation of BMSCs with RAW-β-TCP conditioned medium produced a significant downregulation on the gene expression of osteogenesis-related markers (Runx2, ALP, COLL I, BSP, OCN and BMP-2) compared to cells cultured with RAW-CDHA extracts (Figure 6A, top graph). The incubation with RAW-CDHA extracts resulted in upregulation of Runx2 and BSP compared to that in BMSCs+ group. No significant impact on mineralization was observed showing similar ability of BMSCs to generate calcium deposits and nodule formation, irrespective of the RAW-CaP extract stimulation (Figure 6B).

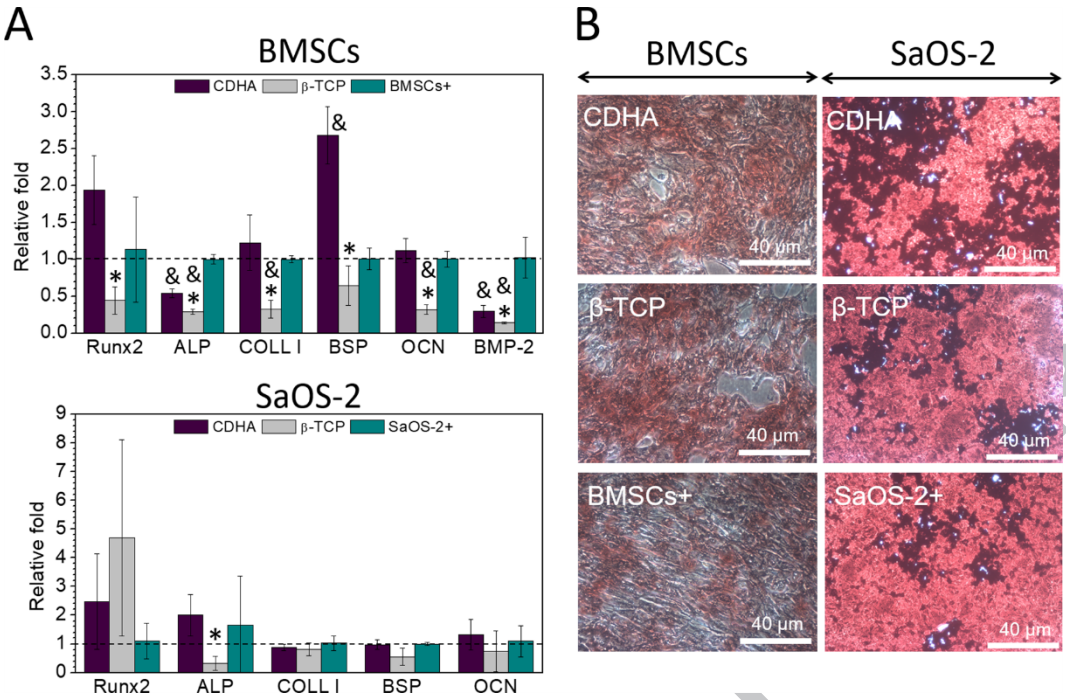

Figure 6. The impact of osteoimmune environment on osteogenesis. **A)** The effect of CaPs-RAW extracts on osteogenic gene expression of BMSCs (top) and SaOS-2 (bottom), respectively. The values of gene expression were normalised to 18S as a housekeeping gene and corresponding BMSCs+ and SaOS-2+ groups were used as a calibrator sample. The dashed line indicates the relative fold equal to 1. * and & indicate statistically significant difference ($p<0.05$) compared to CDHA and corresponding control group (either BMSCs+ or SaOS-2+), respectively. The "BMSCs+" and "SaOS-2+" indicates cells incubated with extracts from LPS-stimulated RAW cells. **B)** The effect of CaPs-RAW conditioned medium on mineralization of BMSCs (left) and SaOS-2 (right).

Compared with the primary cells (BMSCs), SaOS-2 cells showed to be less prone to extract stimulation compared to BMSCs. Incubation with RAW-β-TCP extract resulted in an increase of Runx2 gene expression and a decrease of BSP, OCN and ALP levels, being statistically significant only for ALP (Figure 6B, bottom). Noteworthy, expression of BMP-2 was not

detected for SaOS-2 cells. In general, little upregulation of osteogenic markers was observed for RAW-CaP extracts compared to SaOS-2+. Moreover, ostoblastic cells presented a more intensive staining with Alizarin Red suggesting higher deposition of calcium and formation of nodule compared to BMSCs (Figure 6B). No differences in terms of mineralization were detected for ostoblastic cells incubated with either RAW-β-TCP or RAW-CDHA extract. For the condition where SaOS-2 were cultured directly on the CaPs discs, the CaP-RAW-extracts downregulated some of early osteogenic markers (ALP, BSP). Instead, the late osteogenic marker (OCN) was upregulated by incubation with both CaP- and CaP-RAW conditioned medium (Figure S2).

In general, the effect of RAW-CaP extracts on the ostoegenesis of SaOS-2 cells was more pronounced in protein (Runx2, ALP and COLL I) content evaluated through western blot (Figure 7C and D). Overall, the production of the three measured proteins was significantly higher in SaOS-2 cells stimulated with RAW-CaP conditioned medium compared to cells incubated with extracts from LPS-stimulated RAW cells (SaOS-2+) (Figure 7D). Moreover, the secretion of COLL I by SaOS-2 cells was more pronounced after incubation with RAW-CDHA extracts. Additionally, the ALP protein expression was visualised using CLSM technique (Figure 7A). The cell spreading area was higher in SaOS-2 cells cultured with RAW-CDHA extract compared to SaOS-2+ group (Figure 7B, left graph). No impact of RAW-CaP conditioned medium on SaOS-2 elongation ratio was observed (Figure 7B, right graph).

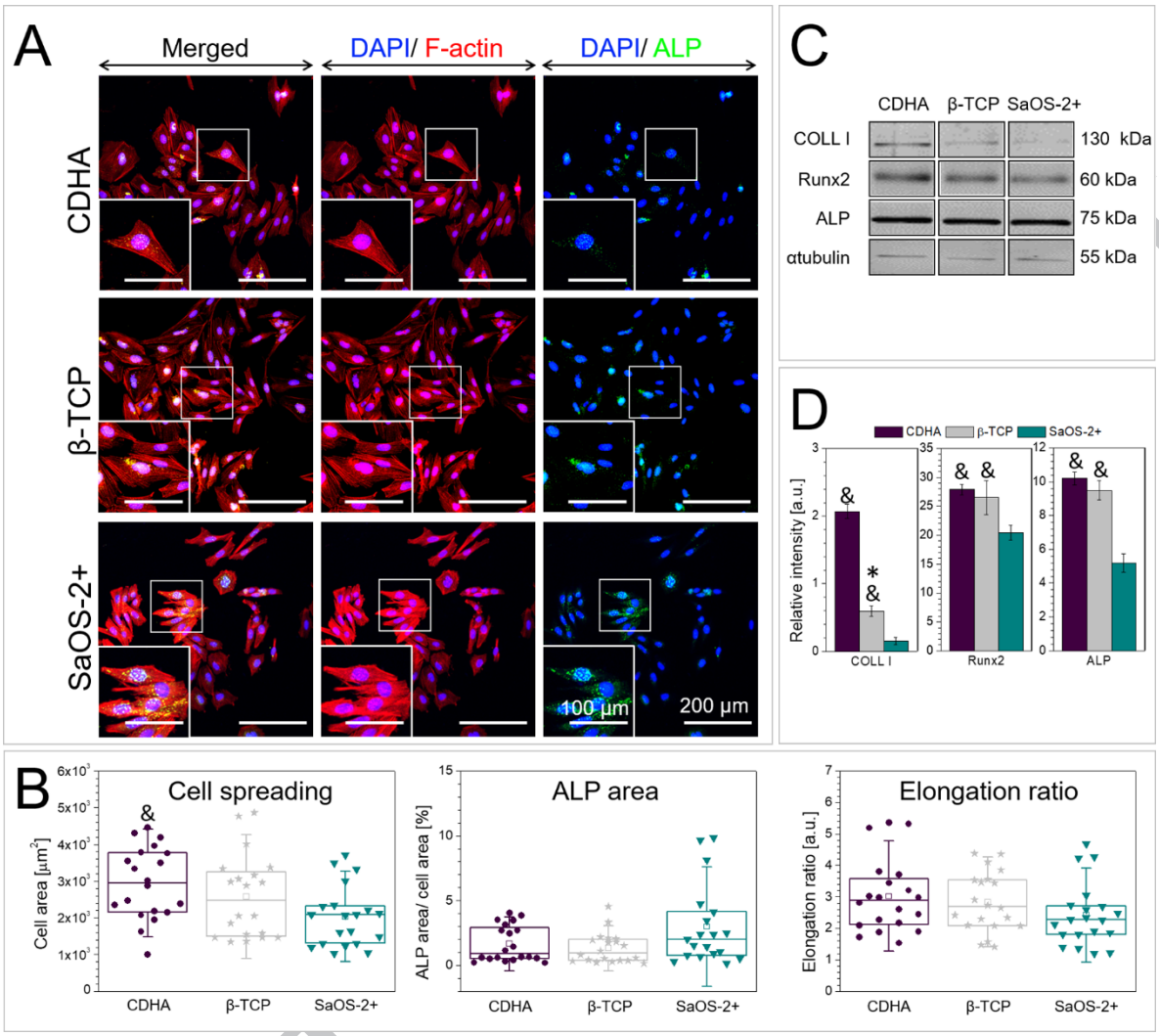

Figure 7. The effect of CaPs-RAW - extracts on protein expression and morphology of SaOs-2 cells. **A)** Representative CLMS images of SaOS-2 after 3 day exposure to CaPs-RAW extracts. The F-actin (red), cellular nuclei (blue) and ALP (green) were stained. The brightness and contrast of images was adjusted with Fiji/Image-J package. **B)** Semiquantitative analysis of SaOs-2 spreading, ALP occupied area and elongation ratio. Symbols represent individual cells (n=20), the boxes represent 25th and 75th percentile, the middle line is the median, the □ is the mean and whiskers are standard deviation. * indicates statistically significant difference ($p<0.05$) compared to SaOS-2+. No significant differences were observed between substrates. **C)** The Western blot of proteins related to osteogenesis (COLL I, Runx2, ALP) detected by Western blot

D) Corresponding relative intensity of Western Blot bands. & indicates statistically significant difference ($p<0.05$) compared to control+. * indicates statistically significant difference ($p<0.05$) compared to CDHA. In all figures, "SaOS-2 +" represents cells incubated with extracts from LPS stimulated RAW cells.

4. DISCUSSION

The capacity of biomaterials to modulate macrophage polarisation has been object of different studies [2,16,18,20–22,53–55]. In the field of synthetic bone grafts this is especially relevant, since tunning the inflammatory response may allow fostering the osteogenic properties of these materials. The present work addressed the interactions of two different bone substitutes, namely β-TCP and CDHA with immune cells. Although the elemental composition of these two compounds is identical, both having a Ca/P ratio of 1.5, the different synthetic routes followed in each case, *i.e.* biomimetic precipitation for CDHA and high-temperature sintering for β-TCP, result in different crystal structure, surface topography, roughness and specific surface area (Figure 1) [50]. The RAW 246.7 cell line was used as a model to study CaPs influence on immune cells response. The analysis of cell number revealed that both CaPs supported adhesion and proliferation of macrophages (Figure 2), in agreement with previous studies [56]. This is particularly important as the accumulation of macrophages at early stage of inflammation is a contributing factor to wound repair [57]. Although CDHA caused a decrease of Ca^{2+} concentration in the cell culture medium, associated to the maturation of the apatitic phase, as reported previously for this type of material [54], the small sample size mitigated the extent of the ionic fluctuations, reducing the impact in cell proliferation [48,50,59,60]. In this respect, it is important to highlight that the maturation of CDHA, which involves the evolution from its

calcium-deficient nature to a more stoichiometric form is a long-term process that occurs progressively when the biomimetic substrate is exposed to cell culture medium [48]. Therefore, no significant changes in the substrate composition are expected in the short cell culture times analysed in this study. Although immune cells have been reported to be sensitive to the textural features of the substrate, previous studies showed that the impact was rather in the phenotypic switch [3,61] and cytokine release [18,19,62] than in cell proliferation.

In order to assess the anti-inflammatory capacity of CaPs, macrophages were firstly stimulated with LPS. This molecule of bacterial origin activates pro-inflammatory M1 phenotype [63] and cytokine release [64] and is commonly used in inflammation related studies [65]. The induction of the pro-inflammatory state was confirmed by the presence of iNOS-positively stained cells for both CaP substrates (Figure 3B). Interestingly, the cells cultured on β-TCP exhibited a significantly higher reduction of iNOS area (Figure 3C, middle graph). Moreover, although both biomimetic CDHA and sintered β-TCP significantly downregulated the gene expression and release of pro-inflammatory cytokines compared to LPS-stimulated RAW cells (control+) (Figure 3A and 3B), the reduction was more pronounced for β-TCP in four out of the six analysed genes involved in the inflammatory process. We hypothesize that the enhanced suppression of pro-inflammatory state by β-TCP is likely due to reduced levels of iNOS. For instance, Chamberlain et al. suggested a close relation between the reduction of local pro-inflammatory response and low levels of nitric oxides [66]. Nevertheless, one should remember that the immunomodulatory effects of the substrates also depends strongly on the condition to which immune cells are exposed. Thus, the expression of inflammatory cytokines vary either if the cells are stimulated with LPS (Figure 3A) or cultured under non-inflammatory environment (Figure S1) [41].The inflammatory activation of macrophages is normally associated to

morphological changes [63]. Whereas the anti-inflammatory M2 phenotype is usually characterised by a more elongated aspect [9,52]. Pro-inflammatory macrophages exhibit rounded-like shapes accompanied with an enlargement of the spreading area [9,67] The SEM images revealed an heterogeneous profile of the macrophages cultured on CDHA and β-TCP, with presence of both M1-like and M2-like morphological features (Figure 4). Although no significant differences were found in terms of the elongation ratio (Figure 3C, bottom graph), RAW cells presented smaller spreading areas on the CaP substrates compared to control+ (Figure 3C, upper graph), which can be related to the downregulation of pro-inflammatory cytokines by CaPs (Figure 3A).

Beyond the immune reaction, the macrophages are known to control osteogenesis and osteoclastogenesis through the release of a wide range of molecules. For instance, several studies underlined the importance of macrophages population for induction of the MSC-based bone regeneration. Specifically, an increased mobilization of immune cells was observed on CaP substrates with transplanted MSCs prior to MSC-mediated ectopic bone formation [68,69]. Moreover, macrophages, as osteoclast precursor cells, can exhibit some osteoclastic-like activity, such as the expression of osteoclastic enzymes, or the capacity to resorb CaP substrates [39]. Although previous studies reported a stimulatory effect of CDHA chemistry and topography osteoclastic differentiation [35,39], we observed little osteoclastic actions of RAW cells in contact with CDHA or with β-TCP. For instance, no actin rings were observed in the multinucleated RAW cells (Figure 5C, right graph), a morphological feature of osteoblastic-like cells through which they create sealed regions that can be subjected to acidic resorption [70], Likewise, no signs of degradation were found in the CaP substrates (Figure 5C, left graph), the microstructure of the substrate remaining intact in the cell-biomaterial interphases. There was no

evidence either of ionic alterations, like an increase of calcium concentration in the cell culture medium, which might have been the result of the resorptive activity of cells (Figure 5B) [35,39]. Moreover, little differences were observed in the expression of osteoclastogenic molecules (CTSK, CAR2 and MMP9) (Figure 5A). Even though osteoclastic response of macrophages to bone grafts can be observed at short time of cell culture [33,39], we hypothesize that the incubation of RAW cells with the CaP substrates without any additional stimulation prevented them from revealing their putative osteoclastic nature. Indeed, the RAW cells do not represent fully functional osteoclastic cells [71]. The full differentiation of monocytes/macrophages to osteoclasts, and hence specific osteoclastic behaviour can be only triggered through contact with stimuli such as OPG, RANKL, and M-CSF [72].

The crosstalk between immune cells and the bone forming cells is essential to complete the inflammation stage and to initiate the new bone formation. Here, we studied the simultaneous effect of secreted molecules from RAW cells cultured on CaPs and the ionic environment produced by the interaction of the CaP substrates with the cell culture medium, on the osteogenic differentiation of mesenchymal and osteoblastic cells (Figure 6 and 7). The exposure of BMSCs to CDHA-RAW conditioned medium resulted in higher values of Runx2 and BSP (Figure 6). This result is particularly interesting inasmuch as CDHA activated in more pronounced manner the expression of pro-inflammatory cytokines by macrophages compared to β-TCP (Figure 3A), which would be expected to result in attenuated osteogenic gene expression by bone forming cells [73,74]. However, some studies have underlined that the proper combination of pro-inflammatory molecules, e.g. IL-1β and TNFα, might also lead to enhanced osteogenic differentiation as well as formation of calcium deposits and nodules [12,75,76]. Another interesting fact is that RAW cultured on CDHA simultaneously expressed higher levels of anti-

inflammatory IL-10 and CD206 compared to β-TCP, which was previously associated with M2b macrophages-a subtype of anti-inflammatory immune cells [77]. Unlike Chen *et al*. we did not notice enhanced osteogenesis of BMSCs after incubation with β-TCP-RAW conditioned medium [78]. We hypothesize that this should be likely associated with different form of β-TCP (powder vs bulk material) and subsequent different interaction with cell culture medium and immune cells. In our previous work we demonstrated that incubation of MSCs with extracts from bulk CaPs, and thus exposing them to CDHA-conditioned environment, was not sufficient stimulus to induce differentiation of MSCs into osteoblastic lineage [50]. Therefore, we hypothesize enhanced osteogenic differentiation of BMSCs observed in current study should be associated with the release of osteogenic and inflammatory stimuli from macrophages cultured on CDHA substrates rather than with the microenvironment created by bulk CaPs after immersion in cell culture medium.

Finally, we assessed the effect of RAW-CaPs osteoimmune environment on more reliable osteoblast cell line *i.e.* SaOS-2. In general, osteoblastic gene expression of SaOS-2 was not significantly affected when exposed to the RAW cells supernatants, except in the case of downregulation ALP for the β-TCP-RAW extract compared to CDHA-RAW extract (Figure 6A). This is in agreement with previous findings that demonstrated that SaOS-2 cells are less prone to the microenvironmental changes compared to mesenchymal stem cells [50, 79]. CLMS image semiquantitative analysis showed enhanced cell spreading [80] after exposure to RAW-CDHA supernatants, what might suggest greater capacity of microenvironment created by this substrate to induce osteogenic differentiation (Figure 7A and B) [80]. Moreover, the effect of osteoimmune environment was reflected in protein expression (Runx2, COLL I and ALP) (Figures 7C and D). The results agree with those obtained for BMSCs, showing that more

favourable environment for osteogenesis is obtained when immune cells are cultured on biomimetic CDHA. Overall, a stimulatory effect was observed when osteoblastic cells were cultured with extracts from macrophage's cultured on CaPs (Figure 6 and 7), a phenomenon previously observed [78]. We initially studied this condition to analyse the effect of macrophages on osteoblastic differentiation without considering the stimulatory effect of CaPs [48,50]. Interestingly, when osteoblastic cells were cultured directly on the CaPs and with extracts from activated macrophages (Figure S2), osteoblastic cells differentiated earlier suggesting a synergistic effect of CaP and cytokines released from macrophages. Nonetheless, better comprehending of this relation requires further *in vitro* investigation of signalling pathways responsible for enhanced osteogenic differentiation of bone forming cells. Therefore, further *in vivo* testing designed to study the interaction between immune and bone cells should be performed to fully support driven hypothesis.

5. CONCLUSIONS

In general, sintered β- TCP reduced to greater extent the release of inflammatory cytokines compared to biomimetic CDHA. Nonetheless, the microenvironment created after culturing macrophages on CDHA showed more potent osteogenic effects, fostering osteogenic differentiation of both BMSC and SaOS-2 cells. Overall, the results from the present work demonstrated that calcium phosphates with different chemical and textural properties modulate differently the immune cell response. This opens the door to new strategies to design smart cell-instructive biomaterials that adapt their performance during all stages of bone healing process from early inflammatory phase to bone remodelling.

Acknowledgments

The authors acknowledge the Ministerio de Ciencia, Innovación y Universidades of the Spanish Government for financial support through MAT2015-65601-R project, co-funded by the EU through European Regional Development Funds and the FPI scholarship of JMS, the Prince Charles Hospital Research Foundation, Guangdong Science and Technology International Cooperative Fund with Queensland University of Technology,. They also thank the Generalitat the Catalunya for funding through project 2017SGR-1165. MPG acknowledges the ICREA Academia award by the Generalitat de Catalunya.

Data statement

The raw/processed data required to reproduce these findings cannot be shared at this time as the data also forms part of an ongoing study.

References

[1] S. Franz, S. Rammelt, D. Scharnweber, J.C. Simon, Immune responses to implants – A review of the implications for the design of immunomodulatory biomaterials, Biomaterials. 32 (2011) 6692–6709.

[2] Z. Chen, T. Klein, R.Z. Murray, R. Crawford, J. Chang, C. Wu, et al., Osteoimmunomodulation for the development of advanced bone biomaterials, Mater. Today. 19 (2016) 304–321.

[3] Z. Chen, A. Bachhuka, F. Wei, X. Wang, G. Liu, K. Vasilev, Y. Xiao, Nanotopography-based strategy for the precise manipulation of osteoimmunomodulation in bone regeneration, Nanoscale. 9 (2017) 18129–18152.

[4] Z. Chen, C. Wu, Y. Xiao, Convergence of Osteoimmunology and Immunomodulation for the Development and Assessment of Bone Biomaterials, in: Immune Response to Implant.

Mater. Devices, Springer International Publishing, Cham, 2017: pp. 107–124.

[5] Y.K. Jong, D. Khang, E.L. Jong, T.J. Webster, Decreased macrophage density on carbon nanotube patterns on polycarbonate urethane, J. Biomed. Mater. Res. - Part A. 88 (2009)

[6] J.M. Anderson, A. Rodriguez, D.T. Chang, Foreign body reaction to biomaterials, Semin. Immunol. 20 (2008) 86–100.

[7] R.D. Devlin, S. V. Reddy, R. Savino, G. Ciliberto, G.D. Roodman, IL-6 mediates the effects of IL-1 or TNF, but not PTHrP or 1,25(OH)2D3, on osteoclast-like cell formation in normal human bone marrow cultures, J. Bone Miner. Res. 13 (1998) 393–399.

[8] M.H. Abdel Meguid, Y.H. Hamad, R.S. Swilam, M.S. Barakat, Relation of interleukin-6 in rheumatoid arthritis patients to systemic bone loss and structural bone damage, Rheumatol. Int. 33 (2013) 697–703.

[9] R. Sridharan, A.R. Cameron, D.J. Kelly, C.J. Kearney, F.J. O'Brien, F.J.O. Brien, Biomaterial based modulation of macrophage polarization: A review and suggested design principles, Mater. Today. 18 (2015) 313–325.

[10] A.C. Wu, L.J. Raggatt, K.A. Alexander, A.R. Pettit, Unraveling macrophage contributions to bone repair, Bonekey Rep. 2 (2013) 1–7.

[11] P. Guihard, Y. Danger, B. Brounais, E. David, R. Brion, J. Delecrin, C.D. Richards, S. Chevalier, F. Rédini, D. Heymann, H. Gascan, F. Blanchard, Induction of osteogenesis in mesenchymal stem cells by activated monocytes/macrophages depends on oncostatin M signaling, Stem Cells. 30 (2012) 762–772.

[12] L. Rifas, T-cell cytokine induction of BMP-2 regulates human mesenchymal stromal cell differentiation and mineralization, J. Cell. Biochem. 98 (2006) 706–714.

[13] S. Han, Z. Chen, P. Han, Q. Hu, Y. Xiao, Activation of Macrophages by Lipopolysaccharide for Assessing the Immunomodulatory Property of Biomaterials, Tissue Eng. Part A. 23 (2017) 1100–1109.

[14] Y. Arima, H. Iwata, Effect of wettability and surface functional groups on protein adsorption and cell adhesion using well-defined mixed self-assembled monolayers, Biomaterials. 28 (2007) 3074–3082.

[15] N. Faucheux, R. Schweiss, K. Lützow, C. Werner, T. Groth, Self-assembled monolayers with different terminating groups as model substrates for cell adhesion studies, Biomaterials. 25 (2004) 2721–2730.

[16] R.J. Schutte, A. Parisi-Amon, W.M. Reichert, Cytokine profiling using monocytes/macrophages cultured on common biomaterials with a range of surface chemistries, J. Biomed. Mater. Res. - Part A. 88 (2009) 128–139.

[17] J.E. McBane, L.A. Matheson, S. Sharifpoor, J.P. Santerre, R.S. Labow, Effect of polyurethane chemistry and protein coating on monocyte differentiation towards a wound healing phenotype macrophage, Biomaterials. 30 (2009) 5497–5504.

[18] Z. Chen, A. Bachhuka, S. Han, F. Wei, S. Lu, R.M. Visalakshan, K. Vasilev, Y. Xiao, Tuning Chemistry and Topography of Nanoengineered Surfaces to Manipulate Immune Response for Bone Regeneration Applications, ACS Nano. 11 (2017) 4494–4506.

[19] S.N. Christo, A. Bachhuka, K.R. Diener, A. Mierczynska, J.D. Hayball, K. Vasilev, The Role of Surface Nanotopography and Chemistry on Primary Neutrophil and Macrophage Cellular Responses, Adv. Healthc. Mater. 5 (2016) 956–965.

[20] S. Chen, J.A. Jones, Y. Xu, H.Y. Low, J.M. Anderson, K.W. Leong, Characterization of topographical effects on macrophage behavior in a foreign body response model, Biomaterials. 31 (2010) 3479–3491.

[21] P.C.S. Bota, A.M.B. Collie, P. Puolakkainen, R.B. Vernon, E.H. Sage, B.D. Ratner, P.S. Stayton, Biomaterial topography alters healing in vivo and monocyte/macrophage activation in vitro, J. Biomed. Mater. Res. - Part A. 95 A (2010) 649–657.

[22] B. Wójciak-Stothard, A. Curtis, W. Monaghan, K. Macdonald, C. Wilkinson, Guidance and activation of murine macrophages by nanometric scale topography, Exp. Cell Res. 223 (1996) 426–435.

[23] H. Yuan, M. Van Den Doel, S. Li, C.A. Van Blitterswijk, K. De Groot, J.D. De Bruijn, A comparison of the osteoinductive potential of two calcium phosphate ceramics implanted intramuscularly in goats, J. Mater. Sci. Mater. Med. 13 (2002) 1271–1275.

[24] A. Barradas, H. Yuan, C. van Blitterswijk, P. Habibovic, Osteoinductive biomaterials: current knowledge of properties, experimental models and biological mechanisms, Eur. Cells Mater. 21 (2011) 407–429.

[25] A. Barba, A. Diez-Escudero, Y. Maazouz, K. Rappe, M. Espanol, E.B. Montufar, M. Bonany, J.M. Sadowska, J. Guillem-Marti, C. Öhman-Mägi, C. Persson, M.C. Manzanares, J. Franch, M.P. Ginebra, Osteoinduction by Foamed and 3D-Printed Calcium Phosphate Scaffolds: Effect of Nanostructure and Pore Architecture, ACS Appl. Mater. Interfaces. 9 (2017) 41722–41736.

[26] A. Barba, Y. Maazouz, A. Diez-Escudero, K. Rappe, M. Espanol, E.B. Montufar, C. Öhman-Mägi, C. Persson, P. Fontecha, M.-C. Manzanares, J. Franch, M.-P. Ginebra, Osteogenesis by foamed and 3D-printed nanostructured calcium phosphate scaffolds: Effect of pore architecture, Acta Biomater. 79 (2018) 135–147.

[27] A. Barba, A. Diez-Escudero, M. Espanol, M. Bonany, J.M. Sadowska, J. Guillem-Marti, C. Öhman-Mägi, C. Persson, M.-C. Manzanares, J. Franch, M.-P. Ginebra, The impact of biomimicry in the design of osteoinductive bone substitutes: nanoscale matters, ACS Appl. Mater. Interfaces. (2019) acsami.8b20749. doi:10.1021/acsami.8b20749.

[28] W. Habraken, P. Habibovic, M. Epple, M. Bohner, Calcium phosphates in biomedical applications: materials for the future?, Biochem. Pharmacol. 19 (2016) 69–87.

[29] M. Bohner, R.J. Miron, A proposed mechanism for material-induced heterotopic ossification, Mater. Today. 22 (2019) 132–141.

[30] Z. Xia, L.M. Grover, Y. Huang, I.E. Adamopoulos, U. Gbureck, J.T. Triffitt, R.M. Shelton, J.E. Barralet, In vitro biodegradation of three brushite calcium phosphate cements by a macrophage cell-line., Biomaterials. 27 (2006) 4557–65..

[31] G. Mestres, M. Espanol, W. Xia, C. Persson, M.P. Ginebra, M.K. Ott, Inflammatory

response to nano- And microstructured hydroxyapatite, PLoS One. 10 (2015) 1–20.

[32] Y. Shiwaku, L. Neff, K. Nagano, K.I. Takeyama, J. De Bruijn, M. Dard, F. Gori, R. Baron, The crosstalk between osteoclasts and osteoblasts is dependent upon the composition and structure of biphasic calcium phosphates, PLoS One. 10 (2015) 1–17.

[33] A. Bernhardt, M. Schumacher, M. Gelinsky, Formation of Osteoclasts on Calcium Phosphate Bone Cements and Polystyrene Depends on Monocyte Isolation Conditions, Tissue Eng. Part C Methods. 21 (2015) 160–170.

[34] N.L. Davison, B. ten Harkel, T. Schoenmaker, X. Luo, H. Yuan, V. Everts, F. Barrère-de Groot, J.D. de Bruijn, Osteoclast resorption of beta-tricalcium phosphate controlled by surface architecture, Biomaterials. 35 (2014) 7441–7451.

[35] G. Ciapetti, G. Di Pompo, S. Avnet, D. Martini, A. Diez-Escudero, E.B. Montufar, M.-P. Ginebra, N. Baldini, Osteoclast differentiation from human blood precursors on biomimetic calcium-phosphate substrates, Acta Biomater. 50 (2017) 102–113.

[36] A. Diez-Escudero, M. Espanol, E.B. Montufar, G. Di Pompo, G. Ciapetti, N. Baldini, M.-P. Ginebra, Focus Ion Beam/Scanning Electron Microscopy Characterization of Osteoclastic Resorption of Calcium Phosphate Substrates, Tissue Eng. Part C Methods. 23 (2017) 118–124.

[37] S. Samavedi, A.R. Whittington, A.S. Goldstein, Calcium phosphate ceramics in bone tissue engineering: a review of properties and their influence on cell behavior., Acta Biomater. 9 (2013) 8037–45.

[38] P. Humbert, M.Á. Brennan, N. Davison, P. Rosset, V. Trichet, F. Blanchard, P. Layrolle, Immune Modulation by Transplanted Calcium Phosphate Biomaterials and Human Mesenchymal Stromal Cells in Bone Regeneration, Front. Immunol. 10 (2019) 1–15.

[39] Z. Chen, X. Mao, L. Tan, T. Friis, C. Wu, R. Crawford, Y. Xiao, Osteoimmunomodulatory properties of magnesium scaffolds coated with β-tricalcium phosphate, Biomaterials. 35 (2014) 8553–8565.

[40] A. Diez-Escudero, M. Espanol, M. Bonany, X. Lu, C. Persson, M.-P. Ginebra, Heparinization of Beta Tricalcium Phosphate: Osteo-immunomodulatory Effects, Adv. Healthc. Mater. 7 (2018) 1700867.

[41] J.M. Sadowska, F. Wei, J. Guo, J. Guillem-Marti, M.-P. Ginebra, Y. Xiao, Effect of nano-structural properties of biomimetic hydroxyapatite on osteoimmunomodulation, Biomaterials. 181 (2018) 318–332.

[42] M.P. Ginebra, E. Fernández, E. A. P.A. De Maeyer, R.M.H.M. Verbeeck, M.G.G. Boltong, J. Ginebra, F.C. Driessens, J. A. A Planell, E. Fernandez, Setting Reaction and Hardening of an Apatitic Calcium Phosphate Cement, J. Dent. Res. 76 (1997) 905–912.

[43] J.M. Sadowska, J. Guillem-Marti, M.-P. Ginebra, The Influence of Physicochemical Properties of Biomimetic Hydroxyapatite on the In Vitro Behavior of Endothelial Progenitor Cells and Their Interaction with Mesenchymal Stem Cells, Adv. Healthc. Mater. 8 (2019) 1801138.

[44] S. Singh, B.J. Jones, R. Crawford, Y. Xiao, Characterization of a Mesenchymal-Like Stem Cell Population from Osteophyte Tissue, Stem Cells Dev. 17 (2008) 245–254..

[45] S. Mareddy, R. Crawford, G. Brooke, Y. Xiao, Clonal Isolation and Characterization of Bone Marrow Stromal Cells from Patients with Osteoarthritis, Tissue Eng. 13 (2007) 819–829.

[46] C.T. Rueden, J. Schindelin, M.C. Hiner, B.E. Dezonia, A.E. Walter, E.T. Arena, K.W. Eliceiri, ImageJ2: ImageJ for the next generation of scientific image data, BMC Bioinformatics. 18 (2017) 529.

[47] K.J. Livak, T.D. Schmittgen, Analysis of relative gene expression data using real-time quantitative PCR and the 2-ΔΔCT method, Methods. 25 (2001) 402–408.

[48] J.M. Sadowska, J. Guillem-Marti, M. Espanol, C. Stähli, N. Döbelin, M.-P. Ginebra, In vitro response of mesenchymal stem cells to biomimetic hydroxyapatite substrates: A new strategy to assess the effect of ion exchange, Acta Biomater. 76 (2018) 319–332.

[49] A. Diez-Escudero, M. Espanol, S. Beats, M.-P. Ginebra, In vitro degradation of calcium phosphates: Effect of multiscale porosity, textural properties and composition, Acta Biomater. 60 (2017) 81–92.

[50] J.-M. Sadowska, J. Guillem-Marti, E.B. Montufar, M. Espanol, M.-P. Ginebra, Biomimetic Versus Sintered Calcium Phosphates: The *In Vitro* Behavior of Osteoblasts and Mesenchymal Stem Cells, Tissue Eng. Part A. 23 (2017) 1297–1309.

[51] S. V. Dorozhkin, Calcium Orthophosphates in Nature, Biology and Medicine, Materials (Basel). 2 (2009) 399–498.

[52] F.Y. McWhorter, T. Wang, P. Nguyen, T. Chung, W.F. Liu, Modulation of macrophage phenotype by cell shape, Proc. Natl. Acad. Sci. 110 (2013) 17253–17258.

[53] W.G. Brodbeck, Y. Nakayama, T. Matsuda, E. Colton, N.P. Ziats, J.M. Anderson, Biomaterial surface chemistry dictates adherent monocyte/macrophage cytokine expression in vitro, Cytokine. 18 (2002) 311–319.

[54] M.L. Godek, J.A. Sampson, N.L. Duchsherer, Q. McElwee, D.W. Grainger, Rho GTPase protein expression and activation in murine monocytes/macrophages are not modulated by model biomaterial surfaces in serum-containing in vitro cultures, J. Biomater. Sci. Polym. Ed. 17 (2006) 1141–1158.

[55] E.M. Sussman, M.C. Halpin, J. Muster, R.T. Moon, B.D. Ratner, Porous implants modulate healing and induce shifts in local macrophage polarization in the foreign body reaction, Ann. Biomed. Eng. 42 (2014) 1508–1516.

[56] K.R. Fernandes, Y. Zhang, A.M.P. Magri, A.C.M. Renno, J.J.J.P. van den Beucken, Biomaterial Property Effects on Platelets and Macrophages: An in Vitro Study, ACS Biomater. Sci. Eng. 3 (2017) 3318–3327.

[57] S.J. Jenkins, D. Ruckerl, P.C. Cook, L.H. Jones, F.D. Finkelman, N. van Rooijen, A.S. MacDonald, J.E. Allen, Local Macrophage Proliferation, Rather than Recruitment from the Blood, Is a Signature of TH2 Inflammation, Science (80-.). 332 (2011) 1284–1288.

[58] P. Pascaud, R. Bareille, C. Bourget, J. Amédée, C. Rey, S. Sarda, Interaction between a bisphosphonate, tiludronate and nanocrystalline apatite: in vitro viability and proliferation of HOP and HBMSC cells, Biomed. Mater. 7 (2012) 054108.

[59] J. Gustavsson, M.P. Ginebra, J. Planell, E. Engel, Osteoblast-like cellular response to dynamic changes in the ionic extracellular environment produced by calcium-deficient hydroxyapatite., J. Mater. Sci. Mater. Med. 23 (2012) 2509–20.

[60] E. Engel, S. Del Valle, C. Aparicio, G. Altankov, L. Asin, J. a Planell, M.-P. Ginebra, Discerning the role of topography and ion exchange in cell response of bioactive tissue engineering scaffolds., Tissue Eng. Part A. 14 (2008) 1341–51.

[61] M. Bartneck, V.A. Schulte, N.E. Paul, M. Diez, M.C. Lensen, G. Zwadlo-Klarwasser, Induction of specific macrophage subtypes by defined micro-patterned structures, Acta Biomater. 6 (2010) 3864–3872.

[62] N.E. Paul, C. Skazik, M. Harwardt, M. Bartneck, B. Denecke, D. Klee, J. Salber, G. Zwadlo-Klarwasser, Topographical control of human macrophages by a regularly microstructured polyvinylidene fluoride surface, Biomaterials. 29 (2008) 4056–4064.

[63] A. Mantovani, S.K. Biswas, M.R. Galdiero, A. Sica, M. Locati, Macrophage plasticity and polarization in tissue repair and remodelling, J. Pathol. 229 (2013) 176–185..

[64] F. Meng, C.A. Lowell, Lipopolysaccharide (LPS)-induced Macrophage Activation and Signal Transduction in the Absence of Src-Family Kinases Hck, Fgr, and Lyn, J. Exp. Med. 185 (1997) 1661–1670.

[65] W. Zhang, X. Shen, L. Xie, M. Chu, Y. Ma, MicroRNA-181b regulates endotoxin tolerance by targeting IL-6 in macrophage RAW264.7 cells, J. Inflamm. (United Kingdom). 12 (2015) 1–9.

[66] L.M. Chamberlain, K.S. Brammer, G.W. Johnston, S. Chien, S. Jin, Macrophage Inflammatory Response to TiO Nanotube Surfaces, J. Biomater. Nanobiotechnol. 02 (2011) 293–300.

[67] A. Schmidt, E. Caron, A. Hall, Lipopolysaccharide-Induced Activation of 2-Integrin Function in Macrophages Requires Irak Kinase Activity, p38 Mitogen- Activated Protein Kinase, and the Rap1 GTPase, Mol. Cell. Biol. 21 (2001) 438–448.

[68] A.-L. Gamblin, M.A. Brennan, A. Renaud, H. Yagita, F. Lézot, D. Heymann, V. Trichet, P. Layrolle, Bone tissue formation with human mesenchymal stem cells and biphasic calcium phosphate ceramics: The local implication of osteoclasts and macrophages, Biomaterials. 35 (2014) 9660–9667.

[69] P.O. Bagnaninchi, M. Tabrizian, C. Holmes, Motility imaging via optical coherence phase microscopy enables label-free monitoring of tissue growth and viability in 3D tissue-engineering scaffolds, J. Tissue Eng. Regen. Med. 9 (2013) 641–645.

[70] M.G. Sørensen, K. Henriksen, S. Schaller, D.B. Henriksen, F.C. Nielsen, M.H. Dziegiel, M.A. Karsdal, Characterization of osteoclasts derived from CD14+ monocytes isolated from peripheral blood, J. Bone Miner. Metab. 25 (2007) 36–45.

[71] B. ten Harkel, T. Schoenmaker, D.I. Picavet, N.L. Davison, T.J. De Vries, V. Everts, B., The foreign body giant cell cannot resorb bone, but dissolves hydroxyapatite like osteoclasts, PLoS One. 10 (2015) 1–19.

[72] S.L. Teitelbaum, Bone resorption by osteoclasts, Science (80-.). 289 (2000) 1504–1508.

[73] Z. Chen, S. Han, M. Shi, G. Liu, Z. Chen, J. Chang, C. Wu, Y. Xiao, Immunomodulatory effects of mesoporous silica nanoparticles on osteogenesis: From nanoimmunotoxicity to nanoimmunotherapy, Appl. Mater. Today. 10 (2018) 184–193.

[74] Z. Chen, J. Yuen, R. Crawford, J. Chang, C. Wu, Y. Xiao, The effect of osteoimmunomodulation on the osteogenic effects of cobalt incorporated β-tricalcium phosphate, Biomaterials. 61 (2015) 126–138.

[75] F.-H. Lin, J.B. Chang, M.H. McGuire, J.A. Yee, B.E. Brigman, Biphasic effects of interleukin-1β on osteoblast differentiation in vitro, J. Orthop. Res. (2010) n/a-n/a.

[76] J. Ding, O. Ghali, P. Lencel, O. Broux, C. Chauveau, J.C. Devedjian, P. Hardouin, D.

Magne, TNF-α and IL-1β inhibit RUNX2 and collagen expression but increase alkaline phosphatase activity and mineralization in human mesenchymal stem cells, Life Sci. 84 (2009) 499–504.

[77] D.M. Mosser, The many faces of macrophage activation, J. Leukoc. Biol. 73 (2003) 209–212.

[78] Z. Chen, C. Wu, W. Gu, T. Klein, R. Crawford, Y. Xiao, Osteogenic differentiation of bone marrow MSCs by β-tricalcium phosphate stimulating macrophages via BMP2 signalling pathway., Biomaterials. 35 (2014) 1507–18.

[79] Y.-F. Chou, W. Huang, J. C. Y. Dunn, T. A. Miller, and B. M. Wu, The effect of biomimetic apatite structure on osteoblast viability, proliferation, and gene expression., Biomaterials 26 (2005), 285–95.

[80] R. McBeath, D.M. Pirone, C.M. Nelson, K. Bhadriraju, C.S. Chen, Cell Shape, Cytoskeletal Tension, and RhoA Regulate Stem Cell Lineage Commitment, Dev. Cell. 6 (2004) 483–495.

Statement of significance

The field of osteoimmunology highlights the importance of the cross-talk between immune and bone cells for effective bone regeneration. This tight interaction opens the door to new strategies that encompass the development of smart cell-instructive biomaterials which performance covers the events from early inflammation to osteogenesis. The present work links the anti-inflammatory and osteoimmunomodulatory features of synthetic bone grafts to their chemistry and texture, focussing on the cross-talk between macrophages and two major orchestrators of bone healing, namely primary mesenchymal stem cells and osteoblasts. The results emphasize the importance of the microenvironment created through the interaction between the substrate and the immune cells as it can stimulate osteogenic events and subsequently foster bone healing.